Drought conditions, aridity and forest structure control the responses of Iberian holm oak woodlands to extreme droughts: a large-scale remote-sensing exploration in eastern Spain

Moreno-de-las-Heras, M.[1]*, Bochet, E.[2], Vicente-Serrano, S.M.[3], Espigares, T.[4], Molina, M.J.[2], Monleón, V.[5], Nicolau, J.M.[6, 7], Tormo, J.[6, 7], García-Fayos, P.[2]

[1] Mediterranean Environmental Research Group (GRAM), Department of Geography, University of Barcelona, 08001 Barcelona, Spain.

[2] Desertification Research Center (CIDE, CSIC-UV-GV), 46113 Moncada (Valencia), Spain.

[3] Pyrenean Institute of Ecology (IPE-CSIC), Spanish National Research Council (CSIC), 50059 Zaragoza, Spain.

[4] Department of Life Sciences, Universidad de Alcalá, 28871 Alcalá de Henares (Madrid), Spain.

[5] US Forest Service Pacific Northwest Research Station, Corvallis, Oregon 97331, USA.

[6] Department of Agrarian and Environmental Sciences, University of Zaragoza, 22071 Huesca, Spain.

[7] Environmental Sciences Institute of Aragon, University of Zaragoza, 50009 Zaragoza, Spain.

*Corresponding author: Mariano Moreno de las Heras (mariano.moreno@ub.edu)

Abstract. Understanding how Mediterranean forests respond to the increasing frequency of extreme droughts and forest densification is crucial for effective land management in the present context of climate change and land abandonment. We study the responses of Iberian holm oak (*Quercus ilex* L.) woodlands to recent extreme droughts during 2000-2019 along broad gradients of climate aridity and forest structure. To this purpose, we apply large-scale remote-sensing using MODIS EVI as a primary production proxy in 5274 *Q. ilex* sites distributed within a 100,000 km^2 region in eastern Spain. These woodlands were extensively affected by two extreme drought events in 2005 and 2012. Resistance, assessed as the capacity of the ecosystems to maintain primary production during drought, was significantly lower for semi-arid than for sub-humid and dry-transition conditions. Holm oak woodlands located in semi-arid areas of the region showed also poorer resilience to drought, characterized by low capacity to fully recover to their pre-drought production levels. Further, drought intensity and both pre- and post-drought hydric conditions controlled the variations of resistance, recovery and resilience between the two analyzed extreme drought events. Drought effects were particularly negative for dense *Q. ilex* stands under semi-arid climate conditions, where strong competition for scarce water resources reduced drought resistance. The observed drought vulnerability of semi-arid holm oak woodlands may affect the long-term stability of these dry forests. Adaptive management strategies, such as selective forest thinning, may be useful for improving drought responses in these more vulnerable semi-arid woodlands. Conversely, natural rewilding may more appropriately guide management actions for more humid areas, where densely developed *Q. ilex* woodlands show in general a high ability to maintain ecosystem primary production during drought.

Keywords: aridity; drought; ecosystem stability; forest structure; holm oak; resilience.

1. Introduction

Forest ecosystems play a critical role for the maintenance of biodiversity worldwide and the provision of many other ecosystem services, including water cycle regulation, erosion control, habitat creation, carbon sequestration, the production of wood and non-wood market goods and cultural/recreative services (Mori et al., 2017). Environmental data records indicate that the organization and function of these landscapes is rapidly changing under the influence of external drivers, such as increased water shortages and frequency of droughts resulting from climate change (Simonson et al., 2014). Drought effects commonly include the reduction of forest productivity, canopy defoliation, tree mortality and the alteration of natural regeneration patterns (Allen et al., 2015; DeSoto et al., 2020; García-Fayos et al., 2020), which together can induce large changes in the carbon cycle at the forest stand level (Reichstein et al., 2013; Anderegg et al., 2020) and long-term geographical displacement at the forest species level (Benito-Garzón et al., 2008; Ruiz-Labourdette et al., 2012; Mauri et al., 2022).

The Mediterranean basin is currently perceived as a hotspot of climate change (Giorgi, 2006; Doblas-Reyes et al., 2021). Regional air temperatures have increased in this region approx. 1.3ºC since 1920, in comparison with a noticeably smaller worldwide increase of ~0.85ºC for the same period (Guiot and Cramer, 2005; Cramer et al., 2020). The greater atmospheric evaporative demand resulting from temperature rise has also contributed to an increase in the frequency, intensity and duration of droughts, especially during the last 5-6 decades (Vicente-Serrano et al., 2014) and will likely continue to amplify in the future, in light of current climate projections of increased water shortages for the Mediterranean region (Ali et al., 2022). Synchronously, land abandonment and the decline of rural population in this region since the second half of the 20th century have contributed to recent forest expansion and stand densification, particularly in areas of the

northern-shore Mediterranean basin (Lana-Renault et al., 2020). The interactions between land-abandonment patterns and climate change in Mediterranean landscapes can lead to complex ecosystem responses. For example, Astigarraga et al. (2020), in a large-scale exploration along the Iberian Peninsula of changes in forest demography and structure along 1986-2017 concluded that forest density, basal area and tree size have increased since the 1980s due to land abandonment. However, this same study also indicates an aggravation of the negative effects of climate change and greater stand competition due to forest densification since the beginning of the 21st century, resulting in increased growth reductions and tree mortality by severe droughts. How forest ecosystems react in the present context of interactions between increased frequency of extreme droughts and forest densification is, therefore, a question of major importance for land management and adaptation in the Mediterranean region.

Resilience is an emergent property of ecosystems that can be described as their ability to absorb and recover from disturbances , regaining the structure and functions that characterize their stability domains (Gunderson, 2000). Accordingly, forest resilience to extreme drought provides an integrated description of the capacity of these ecosystems to maintain, recover and regain the integrity of their functions during and after the effects of extreme droughts (Lloret et al., 2011; Anderegg et al., 2020). Previous studies indicate that these forest responses to drought depend on complex interactions of multiple intrinsic and extrinsic environmental factors. For example, while tree traits and physiology control drought tolerance, drought intensity and both pre- and post-drought conditions have a primary influence on drought stress and post-drought tree growth legacies, constituting important determinants of resilience (McDowell et al., 2008; Greenwood et al., 2017; Forner et al., 2018). Further, climate aridity, which constraints water availability and forest productivity, can largely increase forest vulnerability to drought, particularly for

local tree populations distributed near the species' aridity tolerance limit (Camarero et al., 2013; Gazol et al., 2017; DeSoto et al., 2020). Forest structure is also likely to affect forest responses to drought. Specifically, intense competition for the use of water due to high tree density has been associated with drought-induced tree mortality (Greenwood and Weisberg, 2008; Xerra-Maluquer et al., 2018; Ogaya et al., 2020).

Forest response to drought is frequently assessed using tree dendrochronological analysis, which offers direct metrics of the effects of climate variability on tree growth (Camarero et al., 2016; Gazol et al., 2017; Sánchez-Salguero et al., 2018). The scope of these tree-ring data explorations is, however, commonly limited to single trees and the forest stand scale. The increasing availability of decadal series of remotely sensed data, such as satellite-driven vegetation indexes that strongly correlate with ecosystem net primary production and tree growth, provide excellent approaches for exploring the response of forest ecosystems to drought at very broad spatial scales (Gazol et al., 2018; Vicente-Serrano et al., 2019). In fact, remote sensing techniques offer unique chances for overcoming the strong spatial limitations that characterize dendrochronological approaches, facilitating fast exploration of forest ecosystems over vast areas and remote regions.

Quercus ilex L. (holm oak) is a drought tolerant evergreen oak that constitutes a keystone species for the provision of ecosystem services in the Mediterranean region (Marañón et al., 2012). In fact, *Q. ilex* woodlands are one of the most conspicuous dryland forests in the western Mediterranean basin, where they have been historically impacted during millennia by human activities (mainly wood consumption for fuel, timber and charcoal production, domestic livestock and dryland agriculture) causing reductions of their range and important changes in their structure, including, among others, forest transformations in intensively used coppice stands (Terradas, 1999; Serrada et al., 2017; Camarero and

Valerio, 2023). Since 1950, however, land abandonment has promoted holm oak densification in the region (Vericat et al., 2011). Species distribution models for the Iberian Peninsula and Europe have identified *Q. ilex* as one of the key forest species that will progressively displace cold-temperate forest species in sub-humid landscapes at medium altitudes (800-1400 m) as a consequence of climate change (Ruiz-Labourdette et al., 2012; Mauri et al., 2022). However, these climate change models also warn that future *Q. ilex* distribution in the Mediterranean basin could also be reduced in drier areas of its present distribution range, where holm oak may be increasingly exposed to water scarcity and the effects of extreme droughts (Mauri et al., 2022). These negative projections are in line with results obtained by recent holm oak stand explorations in semi-arid areas of the Mediterranean region, where the lack of natural regeneration and increased tree decline are emerging as significant problems for their stability (Camarero et al., 2016; Gentiliesca et al., 2017; García-Fayos et al., 2020).

Despite the very conspicuous distribution of holm oak woodlands in the Mediterranean region and the important changes that these dryland forests may experience in the future as a function of climate change and land abandonment, the resilience of *Q. ilex* forests to extreme drought has been scarcely explored at very broad spatial scales. Important knowledge gaps in the analysis of these effects are: (i) the influence of aridity along the full range of climate conditions that govern present *Q. ilex* spatial distribution on the capacity of holm oak woodlands to maintain, recover and regain the integrity of primary production during and after drought; and (ii) the impact that forest density, largely influenced by the legacy of past human use and recent land abandonment, has in these drought responses. In this study, we explore the resilience of Iberian holm oak woodlands to recent extreme droughts during 2000-2019, using a remote sensing approach over broad-scale gradients of climate aridity and forest structure in eastern Spain. We expect

150 to find a major impact of drought characteristics and aridity on the analyzed responses to
151 extreme drought, since these factors have a direct influence on water shortages and
152 drought stress. Specifically, we hypothesize that drought vulnerability of these *Q. ilex*
153 woodlands will increase with climate aridity from sub-humid to semi-arid landscapes. We
154 also expect to find a significant effect of forest structure on drought response, particularly
155 under the most arid conditions of *Q. ilex* distribution, since forest density can largely
156 exacerbate competition for scarce water resources.
157

158 **2. Materials and Methods**

159 **2.1. Study area**

160 The study region extends over 100,000 km^2 in eastern Spain, within the Iberian System
161 and surrounding areas of this mountain range, comprising the headwaters of the Douro,
162 Tagus and Guadiana rivers and extensive areas of the Ebro, Jucar, Turia and Mijares river
163 basins (Fig. 1). The climate can be classified as Mediterranean (Papadakis, 1966), with
164 two rainy periods concentrated in spring (April-June) and autumn (September-
165 November). Mean annual precipitation (MAP) and air temperature are 360-750 mm and
166 9.2-14.2°C, respectively (data derived from Ninyerola et al., 2005). Potential
167 evapotranspiration (PET) is 870-1190 mm (data derived from Trabucco and Zomer,
168 2009). Aridity (Ar), referred in this study as 1-MAP/PET, ranges in the region from 0.25
169 to 0.65 from the wettest, sub-humid conditions to the driest, semi-arid conditions,
170 respectively.
171 We selected a total of 5274 study sites (each 232 × 232 m; these dimensions are
172 determined by the pixel size of the UTM re-projected MODIS product applied later in
173 this study for the calculation of ecosystem production and drought resilience
174 components), distributed within sub-humid (175 sites, Ar 0.25-0.35), dry-transition (3165

sites, Ar 0.35-0.50) and semi-arid (1936 sites, Ar 0.50-0.65) climate conditions. Site selection was developed by applying a GIS-based procedure, validated using high-resolution aerial imagery. Specific site selection methods are detailed in Appendix A. Our study sites comprise holm oak woodlands along the full climate distribution range of *Q. ilex* in the region and a broad variety of forest structure (i.e., tree canopy density) conditions, from closed forests to open woodlands. Active use of these holm oak ecosystems, historically managed as coppice woodlands in the study region, ceased about 70 years ago. In fact, human population in the region has showed a 4-fold decrease since 1950, also leading to large reductions in livestock density, which may have facilitated forest recovery in recent decades (Stellmes et al., 2013; Garcia-Fayos et al. 2020). All study sites were selected without any signs of having been recently managed and no past wildfire activity, at least since 2000. Elevation ranges from 730 to 1470 m above sea level and all sites have flat topography (slope angle is equal or less than 6°). Soils are Mollic Haploxeralfs (Soil Survey Staff, 2014) developed over homogeneous calcareous parent lithology (massive limestones of Jurassic and Cretaceous age). The homogeneous topography and soil/lithology characteristics of the study sites were imposed in the site selection criteria to minimize the influence of environmental factors other than the factors of interest under study (i.e., aridity, forest structure and drought characteristics).

2.2. Drought resilience components

We followed the approach described by Lloret et al. (2011) for the analysis of ecosystem responses to extreme drought, using the following three components (or metrics) of resilience to compare ecosystem primary production before, during and after the effects of a drought event (Fig. 2):

(i) Resistance (Rt, dimensionless), which describes the capacity of an ecosystem to resist the effects of a drought, and is calculated as the ratio of ecosystem production during a drought period (EP_{Dr}) to pre-drought ecosystem production (EP_{PreDr}):

$$R_t = EP_{Dr}/EP_{PreDr} \quad (1)$$

(ii) Recovery (Rc, dimensionless), which describes the performance readjustment, in terms of recovery of production, of an ecosystem after a drought, and is calculated as the ratio of post-drought (EP_{PostDr}) to drought (EP_{Dr}) ecosystem production:

$$R_c = EP_{PostDr}/EP_{Dr} \quad (2)$$

(iii) Resilience (Rs, dimensionless), which describes the ability of an ecosystem to regain pre-drought production performance after a drought, and is calculated as the ratio of post-drought (EP_{PostDr}) to pre-drought ecosystem production (EP_{PreDr}):

$$R_s = EP_{PostDr}/EP_{PreDr} \quad (3)$$

We applied remote sensing estimation of annual net primary production, based on temporal series of the enhanced vegetation index (EVI), to calculate the indices of resilience for extreme drought events of the period 2000-2019. Following recommendations of previous studies (Gazol et al., 2017; Sánchez-Salguero et al., 2018), we used reference periods of 3 years before and after the drought events to determine pre-drought and post-drought mean ecosystem production in the calculation of the Rt, Rc and Rs metrics. The selected length for the reference periods agrees with reported 1-year to 3-year post-drought growth recovery of holm oak and other angiosperm forest species (Anderegg et al., 2015; DeSoto et al., 2020; Gazol et al., 2020) and prevents drought event overlap in the studied data series.

2.3. Remote sensing proxy of ecosystem net primary production

223 The enhanced vegetation index (EVI) is a remote-sensing vegetation index strongly
224 sensitive to leaf phenology, which minimizes the interferences caused by the effects of
225 atmospheric aerosols and the variations of soil background color (Huete et al., 2002).
226 Garbulsky et al. (2013) showed that annual EVI strongly correlates with *Q. ilex* stem
227 diametric increment in holm oak woodlands of Spain (Pearson's $R=0.91$, $p<0.001$), hence
228 providing an excellent proxy of tree growth. Furthermore, Ponce-Campos et al. (2013)
229 showed that the annual integral of EVI values provides an excellent estimator for annual
230 net primary production (ANPP) in woodlands and grasslands worldwide across arid,
231 semi-arid and sub-humid climate conditions. We, therefore, apply annual integral values
232 of the enhanced vegetation index (iEVI) as a proxy of ecosystem production for the
233 analysis of drought resilience components in our holm-oak sites.
234 We compiled two-decadal (2000-2019) series of EVI for all the study sites (16-day
235 temporal resolution) from the MODIS Terra satellite (MOD13Q1 product, collection 6)
236 using the NASA's LP DAAC Data Pool. The data were re-projected to UTM ETRS89
237 Zone 30N (232 m resolution after re-projection) and filtered for the removal of anomalous
238 EVI values (e.g., EVI values affected by snow, ice, clouds and other atmospheric
239 anomalies). We applied a weighted Savitzky-Golay adaptive filtering algorithm (Jönsson
240 and Eklundh, 2004) programmed to use the ancillary MOD13Q1 quality/reliability
241 information as criteria for identifying and filtering anomalous EVI values. The algorithm
242 was run using a window size of 5 data points and 3 iterations.
243 Previous studies have found a close synchronization of MODIS EVI trends with the
244 annual cycles of leaf phenology in Iberian woodlands (Garbulsky et al. 2013; Pasquato et
245 al. 2015). Similarly, annual EVI trends in the studied holm oak sites (Fig. C1 a-b in
246 Appendix C) showed an absolute maximum in June, synchronized with spring
247 production, followed by a summer reduction of EVI, frequently leading to a relative

248 minimum value associated with summer drought, and a late, small growth period until
249 the end of autumn. EVI trends then decrease to reach their absolute minimum values
250 during winter, in late February. Accordingly, the processed EVI data was aggregated in
251 annual phenological cycles (from the beginning of March to the end of February of the
252 next year) to obtain the final iEVI values used as ANPP proxy for the calculation of
253 drought resilience components.
254
255 **2.4. Forest structure and its relationship to the legacy of human use**
256 Tree canopy cover (TC, %) estimations for this study (Fig. 3a) were obtained applying a
257 field-calibrated and validated remote sensing data transformation equation developed
258 using 60-m resolution Normalized Difference Red-Edge 2 index (NDRE2; Barnes et al.,
259 2000) data obtained from a winter-season Sentinel-2 composite image of the region
260 (downloaded from the Copernicus Sentinel-2 Global Mosaic service), and 138 reference
261 (232 × 232 m) holm oak sites with field-validated TC information (Moreno-de-las-Heras
262 et al., 2018) that are distributed within the study area. We selected winter-season NDRE2
263 upon 4 alternative seasonal composite images and 21 alternative vegetation indexes, since
264 winter NDRE2 maximized the correlation with the reference TC data (Pearson's R=0.95;
265 p<0.001). The resulting TC-NDRE2 transformation equation ($TC\ (\%) = 215.9NDRE2 - 24.5$)
266 showed an excellent calibration and validation performance
267 (calibration R^2=0.91, n=84 sites; validation RMSE=6%, n=54 sites). Full details for the
268 development, calibration and validation of the NDRE2-TC transformation equation
269 applied for TC estimation can be found in Appendix B.
270 Under the homogeneous soil/lithological and geomorphological conditions of the study
271 sites (calcareous soil parental material and flat topography), maximum tree canopy cover
272 is limited mainly by climate aridity (Moreno-de-las-Heras et al., 2018; Bochet et al.,

2021). In fact, maximum tree canopy cover (TC_{max}, %) varies non-linearly in the study area from approx. 60% in the driest explored semi-arid conditions to 90-100% in the wettest sub-humid conditions of the analyzed aridity range (Fig. 3a). In order to describe forest structure, we standardized their TC values as a function of TC_{max}, using the Local Deforestation index (Dl, dimensionless, Moreno-de-las-Heras et al., 2018):

$$Dl = {(TC_{max} - TC)}/{TC_{max}} \quad (4)$$

Dl is a forest structure and human disturbance index that is independent of climate aridity and ranges from 0 for sites with well preserved, maximum development of forest cover for the climate conditions of the site ($TC = TC_{max}$), to 1 for treeless ($TC = 0\%$) sites that are entirely deforested.

Our study sites comprise a broad variety of forest structure conditions (Fig. 3b), encompassing from dense *Q. ilex* forests, with tree canopy cover close to their climate development potential (Dl <0.35; 1435 sites), to moderately deforested sites (Dl 0.35-0.65; 2967 sites) and very open sites with a few adult, isolated *Q. ilex* trees (Dl >0.65; 872 sites). These Dl variations are closely related to the intensity of human deforestation in the past, controlled in the study region by the proximity of the sites to the nearest human settlements (Fig. 3c), where traditional human activities were typically nucleated (Moreno-de-las-Heras et al., 2018).

2.5. Drought conditions

The Standardized Precipitation Evapotranspiration Index (SPEI, Vicente-Serrano et al., 2010) is a multiscale drought index that quantifies the hydric conditions (i.e., difference between precipitation and atmospheric evaporative demand) as a standardized variable (zero mean and unit variance) and allows for comparison of drought intensity through time and space, independently of the climate conditions of the comparing sites or regions.

SPEI can be calculated for different moments of the year and using different monthly time scales. Negative SPEI values indicate dry conditions, while positive values indicate wet conditions. SPEI takes values below -0.83 and -1.28 (above 0.83 and 1.28) for moderately and severely dry (wet) conditions with 5- and 10-year return periods, respectively. These threshold values were established by detailed analysis of the distribution of extreme events using long-term (up to 117 years) series of SPEI values for the Iberian Peninsula (González-Hidalgo et al. 2018; Liberato et al., 2021).

We obtained 2000-2019 SPEI data for this study from the Historical Database of Meteorological Drought Indices for Spain (https://monitordesequia.csic.es/). This dataset offers gridded (1.1 km spatial resolution) SPEI data available in NetCDF format for the full territory of peninsular Spain with weekly time resolution since 1961 and up to 48-month timescale, developed using climate data of up to 2269 reference stations of the Spanish Meteorological Agency (Vicente-Serrano et al., 2017).

In order to select an optimal SPEI time and scale for analysis, we applied multilevel Pearson correlations (Hox et al., 2018) between the iEVI values of the sites and a variety of SPEI metrics obtained for different months of the phenological cycle (from March to February) and a variety of time aggregation scales (from 1 to 20 months) through 2000-2019. Site ID was set as random-effects grouping variable in the explored multilevel correlations. We selected July SPEI values with a 10-month timescale to characterize the hydric conditions of the years and further analyses, as this metric maximized the correlation between iEVI and SPEI for our set of 5274 *Q. ilex* sites (Multilevel Pearson's $R=0.47$, $p<0.000$; Fig. C2 in Appendix C). Similarly, Peña-Gallardo et al. (2018), using tree ring data in Iberian holm oak woodlands found a high sensitivity of *Q. ilex* tree growth to July SPEI values with 8-12-month timescale.

To characterize the hydric conditions during drought events and their associated pre-drought and post-drought conditions, we applied for each study site and drought year the (July, 10-month scale) SPEI value of the drought event ($SPEI_{Dr}$) and the corresponding SPEI values of the year immediately before and after the drought event ($SPEI_{PreDr}$ and $SPEI_{PostDr}$, respectively).

2.6. Data analysis

2.6.1. Identification and characterization of extreme drought events

Extreme drought events were identified as those drought years within the analyzed series with mean SPEI values for the full region below -1.28 that produced spatially extensive (at least 40% of the sites), significant reductions in the ecosystem productivity of the studied holm oak woodlands. For each site and year, a significant reduction of ecosystem productivity was defined where iEVI was lower than mean minus one standard deviation iEVI of the previous 3-year period. This drought year selection procedure follows the philosophy of the pointer-year approach (Schweingruber et al., 1990). The applied spatial threshold of 40% site drought affection is in the range of common pointer-year threshold values used for analysis at both the tree and site levels (for example, Gazol et al., 2017; Sánchez-Salguero et al., 2018).

For every site, we calculated the resistance Rt, recovery Rc and resilience Rs metrics of each identified extreme drought event using iEVI as ecosystem production proxy. Cross-correlation of the calculated Rt, Rc and Rs metrics was analyzed using multilevel Pearson correlation, applying drought event as random-effects grouping variable. Differences between extreme drought events in the measured (Rt, Rc and Rs) responses of the studied sites were further characterized and tested using paired t tests.

2.6.2. Controlling factors of holm oak woodland resilience to drought

We used linear mixed-effects models (LMM) to study the controlling factors of the Rt, Rc and Rs holm oak woodland resilience responses to extreme drought. Separate LMMs were built for each of the three components of drought resilience, using aridity (Ar) and forest structure (described using the Local Deforestation index, Dl) as environmental fixed-effects variables. We also included the interaction between aridity and forest structure (Ar:Dl), since the effects of forest structure may change as competition for the use of scarce water resources intensifies with aridity. Pre-drought SPEI ($SPEI_{PreDr}$) and drought event SPEI ($SPEI_{Dr}$) were included in the LMM structure for Rt analysis, while both Rc and Rs models included the pre-drought, drought and post-drought SPEI metrics ($SPEI_{PreDr}$, $SPEI_{Dr}$ and $SPEI_{PostDr}$, respectively) as additional fixed-effects environmental variables. Last, site ID was included in all models as random-effects factor to control for the effects of repeated measures between the extreme drought events included in the analysis. We optimized the model structure comparing model configurations of increased complexity (i.e., number of fixed effects), using the Akaike's Information Criterion (AIC; Akaike, 1974), which provides a trade-off between model complexity and goodness of fit (details in Tables C1, C2 and C3 in Appendix C).

Analysis of residual values of the selected optimal models revealed the presence of significant spatial autocorrelation (SAC) in the data. We applied the Residuals Autocovariate approach (Crase et al., 2012; Bardos et al., 2015) to control for the effects of SAC in the optimal Rt, Rc and Rs models. This approach requires the calculation of a spatial autocovariate from the model residuals (RAC, for residual autocovariate), which is later included in the model structure with the environmental explanatory variables and interaction effects, as an additional fixed effect variable. For the selected configurations of the Rt, Rc and Rs models, we applied focal calculation of RAC values (Crase et al.,

2012) within a 500-m neighborhood. We selected a 500-m distance for RAC calculation since this neighborhood length resulted in the best model performance in terms of SAC reduction. RAC inclusion in the optimal Rt, Rc and Rs models successfully removed SAC, as judged by the analysis of spatial cross-correlograms (Bjornstad and Falck, 2001) in the final model residuals. For the final, SAC corrected models, we determined the standardized coefficients (Std. β) and significance of all (environmental and RAC) fixed effects. We also determined for the final models the marginal (fixed-effects only) and conditional (fixed plus random effects) R^2 (Nakagawa and Schielzeth, 2013).

Data processing and analysis was carried out using R 4.1.1 (R Core Team, 2021).

3. Results

3.1. Extreme drought events: the 2005 and 2012 severely dry episodes

Different dry and wet episodes were identified along the study period, as assessed by the (July, 10-month scale) SPEI values of the study sites (Fig. 4a). Years 2005, 2012 and 2017 can be considered dry (mean SPEI of the sites is lower than -0.83), while years 2004, 2010 and 2013 can be considered wet (mean SPEI of the sites is higher than 0.83). Two severely dry episodes (mean SPEI lower than -1.28) were identified for years 2005 (SPEI -1.99 ±0.21 SD) and 2012 (SPEI -1.57 ±0.23 SD). The 2005 drought event was preceded by a year with moderately wet conditions (SPEI 0.88 ±0.25 SD) and succeeded by a normal year (SPEI -0.53 ±0.38 SD). Differently, the 2012 drought was preceded and succeeded by a normal year (SPEI 0.20 ±0.36 SD) and an exceptionally wet year (SPEI 1.27 ±0.26 SD), respectively.

The 2005 and 2012 severely dry episodes extensively affected holm oak woodlands in the territory (Fig. 4 b-c), producing significant iEVI declines (as compared to the corresponding mean minus one SD iEVI of their precedent, reference 3-year periods) for

90% and 51% of the sites, respectively. The 2005 extreme drought affected homogeneously the holm oak woodlands of the territory (Fig. C3a in Appendix C), while the effects of the 2012 extreme drought were distributed more heterogeneously in space. In fact, inland holm oak woodlands located in western areas of the territory, particularly those of sub-humid and dry-transition climate conditions (Ar 0.25-0.50) lying on the mountain range, were less affected by the 2012 drought than *Q.ilex* woodlands distributed in the central and eastern regions of the territory (Fig. C3b in Appendix C).

The 2005 drought impacted woodland productivity, in terms of iEVI drop, more intensively than the 2012 drought, as evidenced by the drought resistance metric (Rt, Fig. 5a). Conversely, post-drought iEVI increase was significantly stronger for the 2005 drought (Rc, Fig. 5b). However, the studied holm oak woodlands recovered pre-drought iEVI levels following the 2012 drought significantly better than following the 2005 extreme event, as indicated by the drought resilience metric (Rs, Fig. 5c). In fact, the 2012 event showed a very good post-drought response, with 15% of the sites exceeding significantly their pre-drought (mean plus one standard deviation) iEVI levels after drought. Overall, Rt showed a strong negative correlation with Rc (Multilevel Pearson's $R=-0.73$; $p<0.001$). Less strong, positive correlations were found between Rs and both Rt and Rc (0.42 and 0.31, respectively; $p<0.001$).

3.2. Holm oak woodland responses to extreme drought: controlling factors

3.2.1. Rt: controlling factors of woodland resistance to drought

The best model structure for the analysis of the controlling factors of woodland resistance to drought included all the (fixed-term) explanatory variables (Ar, Dl, $SPEI_{PreDr}$, $SPEI_{Dr}$) and interactions (Ar:Dl) originally included in the full model (Table C1 in Appendix C). All these effects remained statistically significant at $p<0.001$ after correcting the optimal

422 model to control for the effects of spatial autocorrelation (Table 1). Aridity (Ar) affected
423 negatively drought resistance. In other words, woodland resistance to the effects of
424 extreme droughts (i.e., the capacity to preserve antecedent, pre-drought primary
425 production levels during drought) decreased along the studied aridity gradient (Table 1;
426 Fig. 6a). In addition, the interaction between Ar and Dl positively affected Rt, so that the
427 effect of forest structure (assessed by the local Deforestation index, Dl) was dependent
428 on the aridity level (Table 1). In fact, although drought resistance was higher for holm
429 oak woodlands with well-preserved forest cover (i.e., closed forest structure with canopy
430 cover near the maximum climate potential of the sites) under sub-humid and dry-
431 transition conditions, this tendency was reversed for woodland sites with semi-arid
432 climate conditions, where Rt decreased with forest density. A boundary was found
433 between these two drought resistance trends at the limit between dry-transition and semi-
434 arid conditions (Ar approx. 0.5, Fig. 6a)
435 Pre-drought SPEI and drought SPEI also affected Rt (Table 1; Fig. 6b). In fact, woodland
436 resistance was negatively affected by the hydric conditions of the antecedent, pre-drought
437 year (i.e., the more positive the $SPEI_{PreDr}$ values, the lower the Rt of the sites) and
438 decreased with the intensity of the drought events (i.e., the more negative the $SPEI_{Dr}$
439 values, the lower the Rt of the sites).
440
441 **3.2.2. Rc: controlling factors of woodland recovery to drought**
442 The best model structure for the analysis of the controlling factors of woodland recovery
443 to the effects of extreme droughts included aridity, forest structure and their interactions
444 (Ar, Dl, and Ar:Dl, respectively) as well as the pre-drought and drought SPEI metrics
445 ($SPEI_{PreDr}$, $SPEI_{Dr}$, respectively) as fixed term explanatory variables (Table C2 in
446 Appendix C). All these environmental effects on Rc, which remained significant at

447 $p<0.001$ after correcting the model for the effects of spatial autocorrelation (Table 1),
448 showed opposite trends to those described for Rt. In fact, woodland recovery to drought
449 (i.e., the increase of primary production after drought) increased along the aridity gradient
450 from sub-humid to semi-arid conditions (Table 1; Fig. 7a). In addition, drought recovery
451 of the studied holm oak sites under sub-humid and dry-transition conditions was stronger
452 for heavily deforested, open woodlands than for closed woodlands with well-preserved
453 forest structure (Table 1; Fig. 7a). These effects of forest structure on Rc were less intense
454 under dry-transition conditions and became neutral for semi-arid holm oak sites.
455 Pre-drought SPEI affected positively drought recovery, while drought year SPEI affected
456 negatively Rc (Table 1; Fig. 7b). In other words, the better the hydric conditions of the
457 pre-drought year (i.e., the more positive the $SPEI_{PreDr}$ values) and the more intense the
458 drought event (i.e., the more negative the $SPEI_{Dr}$ values), the higher is the post-drought
459 increase of woodland primary production (i.e., the higher the Rc of the sites).
460

461 **3.2.3. Rs: controlling factors of woodland resilience to drought**

462 The optimal model structure for the analysis of the controlling factors of woodland
463 resilience to drought included aridity (Ar), drought year SPEI ($SPEI_{Dr}$) and post-drought
464 SPEI ($SPEI_{PostDr}$) as explanatory variables (Table C3 in Appendix C), which remained
465 significant at $p<0.001$ after correcting the model for the effects of spatial autocorrelation
466 (Table 1). Ar negatively affected Rs, reducing the ability of the studied holm oak
467 woodlands to fully recover their pre-drought primary production levels from sub-humid
468 to dry-transition and semi-arid conditions (Table 1; Fig. 7a). Both, drought year SPEI and
469 pre-drought SPEI affected positively Rs (Table 1; Fig. 8b). In fact, full recovery of the
470 pre-drought levels of productivity in the studied woodlands was hindered by drought
471 intensity (i.e., the more negative the $SPEI_{Dr}$ values, the lower the Rs of the sites), but was

boosted by the hydric conditions of the subsequent post-drought year (i.e., the more positive the $SPEI_{PostDr}$ values, the higher the Rs of the sites).

4. Discussion

Two extreme droughts with spatially wide impacts on the productivity of the studied holm oak woodlands were identified along 2000-2019: the 2005 and 2012 events. Vicente-Serrano et al. (2014) in an extensive exploration of drought severity in southern Europe identified the 2005 dry event as the most intense and spatially extensive drought that has affected the Iberian Peninsula between the decades of the 1960s and the 2010s. Accordingly, our results indicate that the extreme drought of 2005 affected almost entirely all *Q. ilex* woodlands analyzed within the 100,000 km^2 study region. Numerous studies have reported large impacts in tree growth and forest productivity caused by this extreme drought event, including canopy decay and tree mortality, particularly for pines and cold-temperate broadleaf species (Sánchez-Salguero et al., 2018; Serra-Maluquer et al., 2018; Gazol et al., 2018). Although the 2012 extreme drought was less intense than the 2005 drought, it also affected a high percentage of holm oak woodlands in the study region. Similarly, previous studies have reported significant effects of the 2012 drought for different *Pinus* and *Quercus* species growing in forests and woodlands within the Iberian Range (Camarero et al., 2016; Forner et al., 2018; García-Barreda et al., 2023).

4.1. Controlling effects of *Q. ilex* woodland responses to extreme drought

Determining how Mediterranean forest ecosystems resist, recover and regain their functionality during and after drought is becoming a major ecological issue for the management of these ecosystems in the present context of climate change and land abandonment. Overall, our results indicate that climate aridity and forest density largely

controlled the resistance and recovery of the analyzed *Q. ilex* woodlands to the effects of the 2005 and 2012 extreme drought events, while the ability to regain their primary production levels after drought was further controlled by aridity.

Drought resistance, which describes the capacity of holm oak woodlands to maintain primary production during drought, decreased with climate aridity, which is in accordance with results from other forest species in Spain (Camarero et al., 2013; Gazol et al., 2017; Sánchez-Salguero et al., 2018). During drought, the maintenance of tree growth and ecosystem primary production is highly dependent on the presence of transient reserves of water resources in deep soil horizons, particularly for Mediterranean woodlands dominated by deep-rooted oak species such as *Q. ilex* (Baldocchi and Xu, 2007; Cubera and Moreno, 2007; Moreno-de-las-Heras et al., 2018). While the presence of these deep reserves of soil water resources is feasible in sub-humid landscapes and, to a major extend, in dry-transition areas, their existence is unlikely under drier, semi-arid conditions, which can explain the impact of aridity on drought resistance in our study region. Further, the denser the holm oak woodlands, the better their production levels were maintained during drought under sub-humid and dry-transition climate, while the opposite was true under semi-arid conditions. These contrasting effects of forest structure can be explained because deep-rooted holm oak trees in densely developed sub-humid and dry-transition stands can facilitate maintaining the pre-disturbance ecosystem primary production levels during drought by accessing deep soil water resources (Moreno-de-las-Heras et al., 2018). Conversely, in semi-arid sites where these soil reserves of water are unlikely, a high stand density can only contribute to strongly increase tree competition for scarce water resources, thus reducing resistance to drought (Astigarraga et al., 2020).

Differently to resistance, drought recovery increased in our holm oak woodlands with climate aridity. This may reflect the strong dependence of productivity in semi-arid ecosystems on the annual variations of water availability, where the lack of between-year reserves of soil water resources typically causes a strong coupling and reactive response of primary production to precipitation variations (Huxman et al., 2004; Poulter et al., 2014; Moreno-de-las-Heras et al., 2018; Vicente-Serrano et al., 2019). Alternatively, phenotypic plasticity and possible local adaptation of semi-arid *Q. ilex* populations (e.g., smaller baseline crowns, greater ability of physiological recovery) may also explain, at least in part, the positive impact of climate aridity on drought recovery. Interestingly, low tree density increased drought recovery in the studied holm oak woodlands under sub-humid and dry-transition climate conditions, while these effects of forest structure tended to disappear under semi-arid conditions. This may be due to rapid, intense growth after drought of dense grass vegetation in open *Q. ilex* woodlands under sub-humid and dry-transition conditions. In fact, perennial grass vegetation, which typically exhibits quick and strong growth responses to precipitation pulses (Garcia et al., 2010; Moreno-de-las-Heras et al., 2015), is an essential component of the open holm oak woodlands under the less dry conditions of the explored climate aridity gradient (Bochet et al., 2021). Contrastingly, tree interspaces in open *Q. ilex* woodlands under semi-arid conditions of the study region are scarcely covered by small woody shrub species (e.g., *Thymus vulgaris*, *Helianthemum violaceum*, *Helianthemum marifolium*, *Genista scorpius*) that have a slow growth response compared to grass vegetation and a rather low contribution to landscape-level net primary production. In this sense, it is important to acknowledge that the net primary production (NPP) proxy applied in this work (MODIS iEVI) not only captures the contribution of the tree layer of vegetation but also the NPP contributions of the underlying shrub and grass components of the studied woodlands.

In spite of the detected strong post-drought recovery of production of semi-arid *Q. ilex* woodlands, these dry ecosystems showed a worse capacity to regain their pre-drought production levels compared to sub-humid and dry-transition *Q. ilex* woodlands. DeSoto et al. (2020) suggested that the higher resilience of drought-affected forests and trees in wetter sites is caused by their higher capacity to resist the initial drought impact and keep their pre-disturbance tree status. In this way, the availability of soil water reserves that largely facilitate the maintenance of ecosystem production during drought in wet sites (Serra et al., 2017; Moreno-de-las-Heras et al., 2018; Preisler et al., 2019) can also play an important role for improving drought resilience under sub-humid and dry-transition climate conditions. In turn, the lack of these soil water reserves in dry sites may explain both the lower resistance and resilience of the analyzed semi-arid woodlands.

We acknowledge that, differently to the observed responses of drought resistance and recovery, resilience was not affected by forest structure in the analyzed *Q. ilex* ecosystems. Consistently, Castagneri et al. (2022) in a recent metanalysis over 166 published studies on the influence of stand-level competition on tree growth responses to drought concluded that tree basal area significantly reduces resistance and increases recovery, but does not affect resilience. For the analyzed semi-arid woodlands, the observed lack of influence of forest density on drought resilience may be due to competition-release compensation effects. In fact, Serra-Maluquer et al. (2018) argued that tree decay and mortality during drought can result in competition release in dense forest stands, so that improved water availability after drought can support relatively high growth rates, potentially compensating for the initial negative effects of forest density on drought resistance. These competition-release compensation effects may also be supported by field observations in densely developed holm oak stands of dry areas distributed in NE Spain (Hoya de Huesca region) reporting severe canopy defoliation and

571 significant stem mortality during the 2005 and 2012 drought events followed by higher
572 than expected post-drought growth (García-Barreda et al., 2023). Differently, for wetter
573 areas distributed in our study region, where higher availability of soil water resources
574 reduce competition and increase resistance to drought, strong post-drought growth in
575 open *Q. ilex* woodlands of both tree and between-tree perennial grass vegetation may
576 compensate the benefits that larger densities of deep-rooted holm oak trees accessing deep
577 soil water resources may have for maintaining landscape-level primary production during
578 drought.
579 Besides the discussed effects of climate aridity and forest structure, drought intensity and
580 both pre- and post-drought hydric conditions also conditioned the analyzed drought
581 responses, explaining to a large extent the observed differences in resistance, recovery
582 and resilience of the sites for the 2005 and 2012 drought events. For example, the 2005
583 event was characterized by higher drought intensity than the 2012 drought, thus resulting
584 in larger woodland productivity reductions. These negative effects of drought intensity
585 on resistance, frequently observed in other forest ecosystems (Gazol et al., 2017;
586 Geenwood et al., 2017; Anderegg et al., 2020), may have also be reinforced for the
587 analyzed *Q. ilex* woodlands by the wet pre-drought hydric conditions that took place
588 immediately before the 2005 drought. Zhang et al. (2021) explain this reinforced effect
589 as a function of structural overshoot, where surplus production caused by wet conditions
590 before drought can largely exceed the biomass that can be later maintained during
591 drought.
592 Contrary to drought resistance, the strength of the post-drought recovery of production in
593 the explored holm oak woodlands was increased by both drought intensity and pre-
594 drought hydric conditions, which overall reflects the common interdependence between
595 drought resistance and post-drought recovery (Lloret et al., 2011; Gazol et al., 2018;

596 Manrique-Alba et al., 2022). More importantly, the ability of the studied woodlands to
597 fully regain their pre-drought production levels was negatively affected by drought
598 intensity and further favored by wet post-drought hydric conditions. These effects can
599 explain the very positive resilience observed for the 2012 drought, where 15% of the sites
600 not only recovered, but significantly improved their pre-drought primary production
601 levels after drought. In fact, while the lower drought intensity of the 2012 event may have
602 limited tree damage, providing better conditions for tree post-drought recovery than for
603 the 2005 drought, the exceptionally wet post-drought hydric conditions that took place in
604 2013 very likely promoted strong vegetation growth after the 2012 drought. Accordingly,
605 Forner et al. (2018), in a dendrometer-based localized study developed within our study
606 region, also highlighted the advantages of the exceptionally wet conditions that took place
607 immediately after the 2012 dry event for improving *Q. ilex* drought resilience.
608
609 **4.2. Implications for the stability and management of *Q. ilex* woodlands**
610 Overall, our results highlight the feasibility and potential of our broad-scale remote
611 sensing approach for monitoring the health and drought vulnerability of forest
612 ecosystems, which can largely facilitate their management in large areas with low
613 availability of field data. We observed a strong control of local climate on drought
614 vulnerability, characterized by contrasted responses to extreme drought of *Q. ilex*
615 woodlands along the explored climate aridity gradient. On one hand, the semi-arid *Q. ilex*
616 woodlands of the region show a low resistance to drought and a poor capacity to further
617 regain their pre-drought ecosystem production levels. On the other hand, *Q. ilex*
618 woodlands in sub-humid and dry-transition areas of the region, where wetter climate
619 conditions may alleviate water stress and competition, show higher resistance and
620 resilience to the effects of drought. Interestingly, several studies point to active holm oak

expansion over sub-humid areas of the present distribution range, where *Q. ilex* positive performance during more frequent and intense dry periods is favoring large compositional shifts displacing less drought tolerant species (Peñuelas and Boada, 2003; Navarro-Cerrillo et al., 2019).

Holm oaks in semi-arid areas operate at the limits of hydraulic safety, which largely explains the emergence of more recurrent *Q. ilex* canopy dieback and tree mortality episodes in the present context of increased aridity and drought frequency (Corcuera et al., 2004; Camarero and Valeriano, 2023). In fact, the observed drought sensitivity that characterizes semi-arid *Q. ilex* woodlands in this study region concurs with previous results obtained from localized field observations, dendrochronological analyses and both experimental and modelling studies. For example, Camarero et al. (2016), in a semi-arid *Q. ilex* forest stand located in the Mijares river basin (east of our study region; MAP ~400 mm), observed very intense reductions of basal area increments accompanied by severe defoliation and stem mortality caused by the 2005 and 2012 drought events. Furthermore, Ogaya and Peñuelas (2021) in a 21-year long rainfall exclusion experiment performed in a less dry holm oak forest of the Prades Mountains (NE Spain; MAP ~600 mm) observed that exclusion of 30% annual precipitation caused large stem growth reductions and increases of tree mortality during dry and hot years of the series, also promoting a progressive replacement of *Q. ilex* by more drought resistant shrub species (e.g., *Phillyrea latifolia* L). Overall, these results are in line with predictions obtained by forest species distribution models that foresee future mismatches, as the climate becomes more arid, between the *Q. ilex* ecological niche and the local climate conditions of semi-arid areas within its present distribution range (Benito-Garzón et al., 2008; Mauri et al., 2022).

Our results indicate that the effects of extreme droughts on primary production can be particularly negative for dense forest stands of semi-arid holm oak woodlands, where

competition for the use of scarce soil water resources may be particularly intense. These more vulnerable dry forests are commonly structured in the study region as dense coppice *Q. ilex* stands formed by multiple vegetative stems sprouting from the root network of aged holm oak individuals that were affected in the past by repeated logging. Their aged root architecture and imbalanced root/shoot ratios, which magnify water competition within multiple stems of the same individuals (Camarero et al., 2016), predispose these coppice semi-arid woodlands to drought-induced tree decay and mortality (Gentilesca et al., 2017; Serrada et al., 2017). Tree density reduction through selective thinning has been proposed as a key adaptive strategy for improving drought responses of Mediterranean forests (Molina et al., 2021). The benefits of thinning have been recently tested in overstocked Mediterranean pine plantations and densely developed holm oak stands, obtaining significant tree growth increases and mortality reductions (Ogaya et al., 2020; Molina et al., 2021; Manrique et al., 2022). Selective forest thinning may play a significant role as adaptive management strategy for improving drought responses of the analyzed semi-arid holm oak forests. Conversely, the favorable responses to drought observed in sub-humid and dry transition areas of the study region, where holm oak woodlands with closed forest structure showed in general a high ability to maintain ecosystem primary production during drought, suggest that management actions in wet areas of the *Q. ilex* climate distribution range may be more appropriately directed to facilitate natural rewilding, including holm oak forest expansion and stand densification.

5. Conclusions

This study applied remote sensing analysis of the responses of landscape-level ecosystem production of Iberian *Q. ilex* woodlands to recent extreme droughts during 2000-2019, including the spatially extensive 2005 and 2012 severely dry events, along broad-scale

671 gradients of climate aridity and forest structure in eastern Spain. Drought resistance and
672 post-drought recovery were controlled by climate aridity and forest structure, which
673 largely regulated resource availability and competition for the use of water. The ability to
674 regain the pre-drought production levels after drought was further negatively affected by
675 climate aridity in these holm oak woodlands. All these responses were also affected by
676 drought intensity and both pre- and post-drought hydric conditions, which controlled the
677 variations of the analyzed *Q. ilex* woodland responses between the 2005 and 2012
678 droughts.
679 Semi-arid *Q. ilex* woodlands, located in dry areas of the explored climate aridity gradient,
680 showed a high sensitivity to extreme drought. Their resistance, assessed as the capacity
681 of the woodlands to maintain primary production during drought, was low. Although
682 these dry ecosystems showed a strong post-drought recovery of production, they also
683 showed a poor resilience, characterized by a low capacity to fully regain their pre-drought
684 production levels. Contrarily, holm oak woodlands in sub-humid and dry transition areas
685 of the study region, where wetter climate conditions may alleviate water stress and
686 competition during dry periods, showed a high resistance and resilience to the effects of
687 droughts. Drought vulnerability was particularly high for dense holm oak stands
688 developed under semi-arid climate conditions, where strong competition for scarce water
689 resources largely reduced the ability of the woodlands to maintain landscape-level
690 ecosystem production during drought.
691 The observed drought vulnerability of *Q. ilex* woodlands under semi-arid climate
692 conditions may affect the long-term stability of these dry ecosystems, particularly in the
693 present context of rapid increases of climate aridity and severity of droughts that is taking
694 place in the Mediterranean region. Selective forest thinning may help, as an adaptive
695 management tool, to reduce drought vulnerability of semi-arid *Q. ilex* woodlands in dry

areas of the territory, particularly for those more densely developed forest stands that show a low resistance to the effects of extreme drought. Conversely, natural rewilding may more appropriately guide management actions for more humid areas of the *Q. ilex* distribution range, where densely developed holm oak woodlands show in general a high ability to maintain ecosystem primary production during drought.

Acknowledgements

We would like to thank the NASA's LP DAAC service and ESA's Copernicus program for providing the MODIS and Sentinel-2 data used in this study. We also thank Luis Cayuela Delgado for statistical advice and two anonymous referees for their thoughtful comments. This work was supported by the caRRRascal project (grant RTI2018-095037-B-I00), funded by MCIN/AEI/10.13039/501100011033 and "ERDF A way of making Europe". Mariano Moreno-de-las-Heras is beneficiary of a Serra Hunter fellowship on Physical and Environmental Geography, funded by Generalitat de Catalunya (UB-LE-9055), and grant 2021SGR00859, awarded by the Agència de Gestió d'Ajuts Universitaris i de Recerca de la Generalitat de Catalunya (SGR2021-2024).

Author contributions

Mariano Moreno-de-las-Heras performed conceptualization, methodology, formal analysis and writing – original draft. Esther Bochet and Patricio García-Fayos performed funding acquisition, project coordination, conceptualization and writing – reviewing & edition. Sergio M. Vicente-Serrano, Tiscar Espigares, Maria J. Molina, Vicente Monleón, José M. Nicolau, and Jaume Tormo performed conceptualization and writing – reviewing & edition.

References

Akaike, H. 1974. A new look at the statistical model identification. IEEE Transactions on Automatic Control: 19, 716-723.

Ali, E., Cramer, W., Carnicer, J., Georgopoulou, E., Hilmi, N.J.M., Le Cozannet, G., Lionello, P. 2022. Mediterranean Region. In: Pörtner, O., Roberts, D.C., Tignor, M., Poloczanska, E.S., Mintenbeck, K., Alegría, A., Craig, M., Langsdorf, S., Löschke, S., Möller, V., Okem, A., Rama, B. (eds.), Climate Change 2022: Impacts, Adaptation and Vulnerability. Contribution of Working Group II to the Sixth Assessment Report of the Intergovernmental Panel on Climate Change. Cambridge University Press, Cambridge, UK, pp. 2233–2272.

Allen, C.D., Breshears, D.D., McDowell, N.G. 2015. On underestimation of global vulnerability to tree mortality and forest die-off from hotter drought in the Anthropocene. Ecosphere, 6:129, https://doi.org/10.1890/ES15-00203.1

Anderegg, W.R., Schwalm, C., Biondi, F., Camarero, J.J., Koch, G., Litvak, M., Wolf, A. 2015. Pervasive drought legacies in forest ecosystems and their implications for carbon cycle models. Science, 346: 528-532.

Anderegg, W.R., Trugman, A.T., Badgley, G., Konings, A.G., Shaw, J. 2020. Divergent forest sensitivity to repeated extreme droughts. Nature Climate Change, 10: 1091-1095.

Astigarraga, J., Andivia, E., Zavala, M.A., Gazol, A., Cruz-Alonso, V., Vicente-Serrano, S.M., Ruiz-Benito, P. 2019. Evidence of non-stationary relationships between climate and forests responses: Increased sensitivity to climate change in Iberian forests. Global Change Biology, 26: 5063-5076.

744 Baldocchi, D.D., Xu, L. 2007. What limits evaporation from Mediterranean oak
745 woodlands – The supply of moisture in the soil, physiological control by plants or the
746 demand by the atmosphere? Advances in Water Resources, 30: 2113-2122.
747 Bardos, D.C., Guillera-Arroita, G., Wintle, B.A. 2015. Valid auto-models for spatially
748 autocorrelated occupancy and abundance data. Methods in Ecology and Evolution, 6:
749 1137-1149.
750 Barnes, E.M., Clarke, T.R., Richards, S.E., Colaizzi, P.D., Haberland, J., Kostrzewski,
751 M., Waller, P., Choi, C., Riley, E., Thompson, T., Lascano, R.J., Li, H., Moran, M.S.
752 2000. Coincident detection of crop water stress, nitrogen status and canopy density
753 using ground-based multispectral data. Proceedings of the 5th International Conference
754 on Precision Agriculture. Precision Agriculture Center, University of Minnesota,
755 Bloomington, USA, pp. 1-15.
756 Benito-Garzón, M., Sánchez de Dios, R., Sainz Ollero, H. 2008. Effects of climate change
757 on the distribution of Iberian tree species. Applied Vegetation Science, 11: 169-178.
758 Bjornstad, O.N., Falck, W. 2001. Nonparametric spatial covariance functions: estimation
759 and testing. Environmental and Ecological Statistics, 8: 53-70.
760 Bochet, E., Molina, M.J., Monleón, V., Espigares, T., Nicolau, J.M., Moreno-de-las-
761 Heras, M., García-Fayos, P. 2021. Interactions of past human disturbance and aridity
762 trigger abrupt shifts in the functional state of Mediterranean holm oak woodlands.
763 Catena, 206: 105514, https://doi.org/10.1016/j.catena.2021.105514
764 Camarero, J.J., Valeriano, C. 2023. Responses of pollarded and pruned oaks to climate
765 and drought: Chronicles from threatened cultural woodlands. Science of the Total
766 Environment, 883: 163680, https://doi.org/10.1016/j.scitotenv.2023.163680

767 Camarero, J.J., Manzanedo, R.D., Sanchez-Salguero, R., Navarro-Cerrillo, R.M. 2013.
768 Growth response to climate and drought change along an aridity gradient in the
769 southernmost *Pinus nigra* relict forests. Annals of Forest Science, 70: 769-780.
770 Camarero, J.J., Sangüesa-Barreda, G., Vergarechea, M. 2016. Prior height, growth, and
771 wood anatomy differently predispose to drought-induced dieback in two
772 Mediterranean oak species. Annals of Forest Science, 73: 341-351.
773 Castagneri, D., Vacchiano, G., Hacket-Pain, A., DeRose, R. J., Klein, T., Bottero, A.
774 2022. Meta-analysis reveals different competition effects on tree growth resistance and
775 resilience to drought. Ecosystems, 25: 30-43.
776 Corcuera, L., Camarero, J.J., Gil-Pelegrín, E. 2004. Effects of a severe drought on
777 *Quercus ilex* radial growth and xylem anatomy. Trees, 18: 83-92.
778 Cramer, W., Guiot, J., Marini, K. 2020. Climate and Environmental Change in the
779 Mediterranean Basin - Current Situation and Risks for the Future. First Mediterranean
780 Assessment Report. Union for the Mediterranean, Plan Bleu, UNEP/MAP, Marseille,
781 France.
782 Crase, B., Liedloff, A.C., Wintle, B.A. 2012. A new method for dealing with spatial
783 autocorrelation in species distribution models. Ecography, 35: 879-888.
784 Cubera, E., Moreno, G. 2007. Effect of single Quercus ilex trees upon spatial and seasonal
785 changes in soil water content in dehesas of central western Spain. Annals of Forest
786 Science, 64: 355-364.
787 DeSoto, L., Cailleret, M., Sterck, F., Jansen, S., Kramer, K., Robert, E.M.R., Aakala, T.,
788 Amoroso, M.A., Bigler, C., Camarero, J.J., Cufar, K., Gea-Izquierdo, G., Gillner, S.,
789 Haavik, L.J., Heres, A., Kane, J.M., Kharuk, V.I., Kitzberger, T., Klein, T., Levanic,
790 T., Linares, J.C., Mäkinen, H., Oberhuber, W., Papadopoulos, A., Rohner, B.,
791 Sangüesa-Barreda, G., Stojanovic, D.B., Suárez, M.L., Villalba, R., Martínez-Vilalta,

J. 2020. Low growth resilience to drought is related to future mortality risk in trees. Nature Communications, 11: 545, https://doi.org/10.1038/s41467-020-14300-5

Doblas-Reyes, F.J., Sörensson, A.A., Almazroui, M., Dosio, A., Gutowski, W.J., Haarsma, R., Hamdi, R., Hewitson, B., Kwon, W.T., Lamptey, B.L., Maraun, D., Stephenson, T.S., Takayabu, I., Terray, L., Turner, A., Zuo, Z. 2021: Linking Global to Regional Climate Change. In Climate Change 2021: The Physical Science Basis. In: Masson-Delmotte, V., Zhai, P., Pirani, A., Connors, S.L., Péan, C., Berger, S., Caud, N., Chen, Y., Goldfarb, L., Gomis, M.I., Huang, M., Leitzell, K., Lonnoy, E., Matthews, J.B.R., Maycock, T.K., Waterfield, T., Yelekçi, O., Yu, R., Zhou, B. (eds.), Contribution of Working Group I to the Sixth Assessment Report of the Intergovernmental Panel on Climate Change, Cambridge University Press, Cambridge, UK, pp. 1363-1512.

Forner, A., Valladares, F., Bonal, D., Granier, A., Grossiord, C., Aranda, I. 2018. Extreme droughts affecting Mediterranean tree species' growth and water-use efficiency: the importance of timing. Tree Physiology, 38: 1127-1137.

Gaitán, E., Monjo, R., Pórtoles, J., Pino-Otín, M.R. 2020. Impact of climate change on drought in Aragón (NE Spain). Science of the Total Environment, 740: 140094, https://doi.org/10.1016/j.scitotenv.2020.140094

Garbulsky, M., Peñuelas, J., Ogaya, R., Filella, I. 2013. Leaf and stand-level carbon uptake of a Mediterranean- forest estimated using the satellite-derived reflectance indices EVI and PRI. International Journal of Remote Sensing, 34: 1282-1296.

García, M., Litago, J., Palacios-Orueta, A., Pinzon, J.E., and Ustin, S.L. 2010. Short-term propagation of rainfall peturbations on terrestrial ecosystems in central California. Applied Vegetation Science, 13: 146-162.

García-Barreda, S., Valeriano, C., Camarero, J.J. 2023. Drought constrains acorn production and tree growth in the Mediterranean holm oak and triggers weak legacy effects. Agricultural and Forest Meteorology, 334: 109435, https://doi.org/10.1016/j.agrformet.2023.109435

García-Fayos, P., Monleón, V.J., Espigares, T., Nicolau, J.M., Bochet, E. 2020. Increasing aridity threatens the sexual regeneration of *Quercus ilex* (holm oak) in Mediterranean ecosystems. PLoS ONE, 15: e0239755, https://doi.org/10.1371/journal.pone.0239755

Gazol, A., Ribas, M., Gutiérrez, E., Camarero, J.J. 2017. Aleppo pine forests from across Spain show drought-induced growth decline and partial recovery. Agricultural and Forest Meteorology, 232: 186-194.

Gazol, A., Camarero, J.J., Vicente-Serrano, S., Sánchez-Salguero, R., Gutiérrez, E., de Luis, M., Sngüesa-Barreda, G., Novak, K., Rozas, V., Tíscar, P.A., Linares, J.C., Martín-Hernández, N., Martínez del Castillo, E., Ribas, M., García-González, I., Silla, F., Camisóm, A., Génova, M., Olano, J.M., Longares, L.A., Hevia, A., Tomás-Burguera, M., Galván, J.D. 2018. Forest resilience to drought varies across biomes. Global Change Biology, 24: 2143-2158.

Gazol, A., Camarero, J.J., Sánchez-Salguero, R., Vicente-Serrano, S., Serra-Maluquer, X., Gutiérrez, E., de Luis, M., Sngüesa-Barreda, G., Novak, K., Rozas, V., Tíscar, P.A., Linares, J.C., Martínez del Castillo, E., Ribas, M., García-González, I., Silla, F., Camisóm, A., Génova, M., Olano, J.M., Heres, A., Curiel Yuste, J., Longares, L.A., Hevia, A., Tomás-Burguera, M., Galván, J.D. 2020. Drought legacies are short, prevail in dry conifer forests and depend on growth variability. Journal of Ecology, 108: 2473-2484.

840 Gentilesca, T., Camarero, J.J., Colangelo, M., Nolè, A., Ripullone, F. 2017. Drought-
841 induced oak decline in the western Mediterranean region: an overview on current
842 evidences, mechanisms and management options to improve forest resilience. iForest,
843 10: 796-806.
844 Giorgi, F. 2006. Climate change hot-spots. Geophysical Research Letters, 33: L08707,
845 https://doi.org/10.1029/2006GL025734
846 González-Hidalgo, J.C., Vicente-Serrano, S.M., Peña-Angulo, D., Salinas, C., Tomas-
847 Burguera, M., Beguería, S. 2018. High-resolution spatio-temporal analyses of drought
848 episodes in the western Mediterranean basin (Spanish mainland, Iberian Peninsula).
849 Acta Geophysica, 66: 381-392.
850 Greenwood, D.L., Weisberg, P.J. 2008. Density-dependent tree mortality in pinyon-
851 juniper woodlands. Forest Ecology and Management, 255: 2129-2137.
852 Greenwood, S., Ruiz-Benito, P., Martínez-Vilalta, J., Lloret, F., Kitzberger, T., Allen,
853 C.D., Fensham, R., Laughlin, D.C., Kattge, J., Bönisch, G., Kraft, N.J.B., Jump, A.S.
854 2017. Tree mortality across biomes is promoted by drought intensity, lower wood
855 density and higher specific leaf area. Ecology Letters, 20: 539-553.
856 Guiot, J., Cramer, W. 2016. Climate change: The 2015 Paris Agreement thresholds and
857 Mediterranean basin ecosystems. Science, 354: 465-468.
858 Gunderson, L.H. 2000. Ecological resilience in theory and application. Annual Review
859 of Ecology and Systematics, 31: 425-439.
860 Hox, J., Moerbeek, M., van de Schoot, R. 2018. Multilevel Analysis: Techniques and
861 Applications (3rd ed.). Routledge, New York, USA.
862 Huete, A., Dida, K., Miura, T., Rodriguez, E.P., Gao, X., Ferreira, L.G. 2002. Overview
863 of the radiometric and biophysical performance of the MODIS vegetation indices.
864 Remote Sensing of the Environment, 83: 195-213.

865 Huxman, T.E., Smith, M.D., Fay, P.A., Knapp, A.K., Shaw, M.R., Loik, M.E., Smith,
866 S.D., Tissue, D.T., Zak, J.C., Weltzin, J.F., Pockman, W.T., Sala, O.E., Haddad, B.M.,
867 Harte, J., Koch, G.W., Schwinning, S., Small, E.E., Williams, D.G. 2004.
868 Convergence across biomes to a common rain-use efficiency. Nature, 429: 651-654.
869 Jönsson, P., Eklundh, L. 2004. TIMESAT – a program for analyzing time-series of
870 satellite sensor data. Computers and Geosciences, 30: 933-845.
871 Lana-Renault, N., Morán-Tejeda, E., Moreno-de-las-Heras, M., Lorenzo-Lacruz, J.,
872 López-Moreno, N. 2020. Land-use change and impacts. In: Zribi, M., Brocca, l.,
873 Tramblay, Y., Molle, F. (eds.), Water Resources in the Mediterranean Region.
874 Elsevier, Amsterdam, The Netherlands, pp. 257-296.
875 Liberato, M.L.R., Montero, I., Gouveia, C., Russo, A., Ramos, A. M., Trigo, R.M. 2021.
876 Rankings of extreme and widespread dry and wet events in the Iberian Peninsula
877 between 1901 and 2016. Earth System Dynamics, 12: 197-210.
878 Lloret, F., Keeling, E.G., Sala, A. 2011. Components of tree resilience: effects of
879 successive low-growth episodes in old ponderosa pine forests. Oikos, 120: 1909-1920.
880 Manrique-Alba, A., Beguería, S., Camarero, J.J. 2022. Long-term effects of forest
881 management on post-drought resilience: An analytical framework. Science of the Total
882 Environments, 810: 152374, https://doi.org/10.1016/j.scitotenv.2021.152374
883 Marañón, T., Ibáñez, B., Anaya-Romero, M., Muñoz-Rojas, M., Pérez-Ramos, I. 2012.
884 Oak trees and woodlands providing ecosystem services in southern Spain. In:
885 Rotherham, I.D., Handley, C., Agnoletti, M., Samojlik, T. (eds.), Trees Beyond the
886 Wood: An Exploration of Concepts of Woods, Forests and Trees. Wildtrack Pub.,
887 Sheffield, UK, pp. 291-299.

888 Mauri, A., Girardello, M., Strona, G., Beck, P.S.A., Forzieri, G., Caudullo, G., Manca,
889 F., Cescatti, A. 2022. EU-Trees4F, a datase ton the future distribution of European tree
890 species. Scientific Data, 9: 37, https://doi.org/10.1038/s41597-022-01128-5
891 McDowell, N., Pockman, W.T., Allen, C.D., Breshears, D.D., Cobb, N., Kolb, T., Plaut,
892 J., Sperry, J., West, A., Williams, D.G., Yepez, E.A. 2008. Mechanisms of plant
893 survival and mortality during drought: why do some plants survive while others
894 succumb to drought? New Phytologists, 178: 719-739.
895 Molina, A.J., Navarro-Cerrillo, R.M., Pérez-Romero, J., Alejano, R., Bellot, J.F., Blanco,
896 J.A., Camarero, J.J., Carrara, A., Castillo, V.M., Cervera, T., Barberá, G.G., González-
897 Sanchis, M., Hernández, A., Imbert, J.B., Jiménez, M.N., Llorens, P., Lucas-Borja,
898 M.E., Moreno, G., Moreno-de-las-Heras, M., Navarro, F.B., Palacios, G., Palero, N.,
899 Ripoll, A.A., Regües, D., Ruiz-Gómez, F.J., Vilagrosa, A., del Campo, A.D. 2021.
900 SilvAdapt.net: A site-based network of adaptive forest management related to climate
901 change in Spain. Forests, 12: 1807, https://doi.org/10.3390/f12121807
902 Moreno-de-las-Heras, M., Díaz-Sierra, R., Turnbull, L., and Wainwright, J. 2015.
903 Assessing vegetation structure and ANPP dynamics in a grassland–shrubland
904 Chihuahuan ecotone using NDVI–rainfall relationships, Biogeosciences, 12: 2907-
905 2925.
906 Moreno-de-las-Heras, M., Bochet, E., Monleón, V., Espigares, T., Nicolau, J.M., Molina,
907 M.J., García-Fayos, P. 2018. Aridity induces nonlinear effects of human disturbance
908 on precipitation-use efficiency of Iberian woodlands. Ecosystems, 21: 1295-1305.
909 Mori, A.S., Lertzman, K.P., Gustafsson, L. 2017. Biodiversity and ecosystem services in
910 forest ecosystems: a research agenda for applied forest ecology. Journal of Applied
911 Ecology, 54: 12-27.

912 Nakagawa, S., Schielzeth, H. 2013. A general and simple method for obtaining R2 from
913 generalized linear mixed-effects models. Methods in Ecology and Evolution, 4: 133-
914 142.
915 Navarro-Cerrillo, R.M., Sarmoum, M., Gazol, A., Abdoun, F., Camarero, J.J. 2019. The
916 decline of Algerian *Cedrus atlantica* forests is driven by a climate shift towards drier
917 conditions. Dendrochronologia, 55: 60-70.
918 Ninyerola, M., Pons, X., Roure, J.M. 2005. Atlas Climático Digital de la Península
919 Ibérica. Metodología y Aplicaciones en Bioclimatología y Geobotánica. Universidad
920 Autónoma de Barcelona, Bellaterra.
921 Ogaya, R., Peñuelas, J. 2021. Climate change effects in a Mediterranean forest following
922 21 consecutive years of experimental drought. Forests, 12: 306,
923 https://doi.org/10.3390/f12030306
924 Ogaya, R., Escolà, A., Liu, D., Barbeta, A., Peñuelas, J. 2020. Effects of thinning in a
925 water-limited holm oak forest. Journal of Sustainable Forestry, 39: 365-378.
926 Papadakis, J. 1966. Climates of the World and their Agricultural Potentialities. Eigenverl.
927 d. Verf., Buenos Aires, Argentina.
928 Pasquato, M., Medici, C., Friend, A.D., Francés, F. 2015. Comparing two approaches for
929 parsimonious vegetation modelling in semiarid regions using satellite data.
930 Ecohydrology, 8: 1024-1036.
931 Peña-Gallardo, M., Vicente-Serrano, S.M., Camarero, J.J., Gazol, A., Sánchez-salguero,
932 R., Domínguez-Castro, F., El Kenawy, A., Buegería-Portugués, S., Gutiérrez, E., de
933 Luis, M., Sangüesa-Barreda, G., Novak, K., Rozas, V., Tíscar, P.A., Linares, J.C.,
934 Martínez del Castillo, E., Ribas Matamoros, M., García-González, I., Silla, F.,
935 Camisón, A., Génova, M., Olano, J.M., Longares, L.A., Hevia, A., Galván, J.D. 2018.

936 Drought sensitiveness on forest growth in Peninsular Spain and the Balearic Islands.
937 Forests, 9: 524, https://doi.org/10.3390/f9090524
938 Peñuelas, J., Boada, M. 2003. A global change-induced biome shift in the Montseny
939 mountains (NE Spain). Global Change Biology, 9: 131-140.
940 Ponce-Campos, G.E., Moran, A.S., Huete, A., Zhand, Y., Bresloff, C., Huxman, T.E.,
941 Eamus, D., Bosch, D.D., Buda, A.R., Gunter, S.A., Scalley, T.H., Kitchen, S.G.,
942 McClaran, M.P., McNab, W.H., Montoya, D.S., Morgan, J.A., Peters, D.P.C., Sadler,
943 E.J., Seyfred, M.S., Starks, P.J. 2013. Ecosystem resilience despite large-scale altered
944 hydro-climatic conditions. Nature, 494: 349-353.
945 Poulter, B., Frank, D., Ciais, P., Myneni, R.B., Bi, J., Broquet, G., Canadell, J.G.,
946 Chevalier, F., Liu, Y.Y., Running, S.W., Stich, S., van der Werf, G.R. 2014.
947 Contribution of semi-arid ecosystems to interannual variability of the global carbon
948 cycle. Nature, 509: 600-603.
949 Preisler, Y., Tatarinov, F., Grünzweig, J.M., Bert, D., Ogée, J., Wingate, L., Rotenberg,
950 E., Rohatyn, S., Her, N., Moshe, I., Klein, T., Yakir, D. 2019. Mortality versus survival
951 in drought-affected Aleppo pine forests depends on the extent of rock cover and soil
952 stoniness. Functional Ecology, 33: 901-912.
953 R Core Team. 2021. R: A language and environment for statistical computing. R
954 Foundation for Statistical Computing, Vienna, Austria. https://www.R-project.org/
955 Reichstein, M., Bahn, M., Ciais, P., frank, D., Mahacha, M.D., Seneviratne, S.I.,
956 Zscheischler, J., Beer, J., Buchmann, N., Frank, D.C., Papale, D., Rammig, A., smith,
957 P., Thonicke, K., van der Velde, M., Vicca, S., Walz, A., Wattenbach, M. 2013.
958 Climate extremes and the carbon cycle. Nature, 500: 287–295.
959 Ruiz-Labourdette, D., Nogués-Bravo, D., Sáinz Ollero, H., Schmitz, M.F., Pineda, F.D.
960 2017. Forest composition in Mediterranean mountains is projected to shift along the

961 entire elevational gradient under climate change. Journal of Biogeography, 39: 162-
962 176.
963 Sánchez-Salguero, R., Camarero, J.J., Rozas, V., Génova, M., Olano, J.M., Arzac, A.,
964 Gazol, A., Caminero, L., Tejedor, E., de Luis, M., Linares, J.C. 2018. Resist, recover
965 or both? Growth plasticity in response to drought is geographically structured and
966 linked to intraspecific variability in *Pinus pinaster*. Journal of Biogeography, 45:
967 1126-1139.
968 Schweingruber, F.H., Eckstein, D., Bachet, S., Bräker, O.U. 1990. Identification,
969 presentation and interpretation of event years and pointer years in dendrochronology.
970 Dendrochronologia, 8: 9-38.
971 Serra-Maluquer, X., Menucuccini, M., Martínez-Vilalta, J. 2018. Changes in tree
972 resistance, recovery and resilience across three successive extreme droughts in the
973 northeast Iberian Peninsula. Oecologia, 187: 343-354.
974 Serrada, R., Gómez-Sanz, V., Aroca, M.J., Otero, J., Bravo-Fernández, J.A., Roig, S.
975 2017. Decline in holm oak coppices (*Quercus ilex* L. subs. *ballota* (Desf.) Samp.):
976 biometric and physiological interpretations. Forest Systems, 26: e06S,
977 https://doi.org/10.5424/fs/2017262-10583
978 Simonson, W.D., Coomes, D.A., Burslem, D.F. 2014. Forests and global change: an
979 overview. In: Simonson, W.D., Coomes, D.A., Burslem, D.F. (eds.), Forests and
980 Global Change. Cambridge University Press, Cambridge, UK, pp. 1-18.
981 Soil Survey Staff. 2014. Keys to Soil Taxonomy, 12th edition. United States Department
982 of Agriculture (USDA), Natural Resources Conservation Service, Washington, USA.
983 Stellmes, M., Röder, A., Udelhoven, T., Hill, J. 2013. Mapping syndromes of land change
984 in Spain with remote sensing time series, demographic and climatic data. Land Use
985 Policy, 30: 685-702.

Terradas, J. 1999. Holm oak and holm oak forests: an introduction. In: Rodà, F., Retana, J., García, C.A., Bellot, J., Terradas, J. (eds.), Ecology of Mediterranean Evergreen Forests. Springer, Berlin, Germany, pp. 3-14.

Trabucco, A., Zomer, R.J. 2009. Global potential evapo-transpiration (Global-PET) dataset. Consortium of International Agricultural Research Centers (CGIAR), Consortium for Spatial Information (CSI).

Vericat, P., Piqué, M., Beltrán, M., Cervera, T. 2011. Models de Gestió per als Boscos d'Alzina i Carrasca: Producció de Fusta i Prevenció d'Incendis Forestals. Centre de la Propietat Forestal, Departament d'Agricultura, Ramaderia, Pesca, Alimentació i Medi Natural, Generalitat de Catalunya. Barcelona, Spain.

Vicente-Serrano, S., Beguería, S., López-Moreno, J.I. 2010. A multiescalar drought index sensitive to global warming: The Standardized Precipitation Evapotranspiration Index. Jornal of Climate, 23: 1696-1718.

Vicente-Serrano, S., López-Moreno, J., Begueria, S., Lorenzo-Lacruz, J., Sánchez-Lorenzo, a., García-Ruiz, J.M., Azorín-Molina, C., Morán-Tejeda, E., Revuelto, J., Trigo, r., Coelho, f., Espejo, F. 2014. Evidence of increasing drought severity caused by temperature rise in southern Europe. Environmental Research Letters, 9: 044001, http://dx.doi.org/10.1088/1748-9326/9/4/044001

Vicente-Serrano, S., Tomas-Burguera, M., Beguería, S., Reig, F., Latorre, B., Peña-Gallardo, M., Luna, M.Y., Morata, A., González-Hidalgo, J.C. 2017. A high resolution dataset of drought indices for Spain. Data, 2: 22, https://doi.org/10.3390/data2030022

Vicente-Serrano, S., Azorín-Molina, C., Peña-Gallardo, M., Tomas-Burguera, M., Domínguez-Castro, F., Martín-Hernández, Beguería, S., El Kenawy, A., Noguera, I., García, M. 2019. A high-resolution spatial assessment of the impacts of drought

1010 variability on vegetation activity in Spain from 1981 to 2015. Natural Hazards and
1011 Earth System Sciences, 19: 1189-1213.
1012 Zhang, Y., Keenan, T.F., Zhou, S. 2021. Exacerbated drought impacts on global
1013 ecosystems due to structural overshoot. Nature Ecology and Evolution, 5: 1490-1498.

Table 1. Linear mixed model results (model fit and fixed effects) for the drought resistance (R_t), recovery (R_c) and resilience (R_s) metrics. All three final models are corrected to control for the effects of spatial autocorrelation using the Residual Autocovariate (Crase et al., 2012; Bardos et al., 2015) approach.

					Resistance (R_t)
Marginal R^2	0.83				
Conditional R^2	0.85				
	St. β	**S.E.**	**d.f.**	***t***	***P***
Environmental variables					
Ar	-0.410	0.012	5270	-35.6	<0.001
Dl	-0.501	0.032	5270	-15.8	<0.001
Ar:Dl	0.465	0.034	5270	13.6	<0.001
$SPEI_{PreDr}$	-0.282	0.005	5271	-64.2	<0.001
$SPEI_{Dr}$	0.397	0.004	5271	85.7	<0.001
Spatial autocovariate					
RAC	0.681	0.004	5271	172.1	<0.001
					Recovery (R_c)
Marginal R^2	0.80				
Conditional R^2	0.81				
	St. β	**S.E.**	**d.f.**	***t***	***P***
Environmental variables					
Ar	0.311	0.012	5270	25.7	<0.001
Dl	0.441	0.033	5270	13.2	<0.001
Ar:Dl	-0.371	0.036	5270	-10.4	<0.001
$SPEI_{PreDr}$	0.278	0.005	5271	57.7	<0.001
$SPEI_{Dr}$	-0.261	0.005	5271	-51.9	<0.001
Spatial autocovariate					
RAC	0.748	0.004	5271	173.0	<0.001
					Resilience (R_s)
Marginal R^2	0.80				
Conditional R^2	0.81				
	St. β	**S.E.**	**d.f.**	***t***	***P***
Environmental variables					
Ar	-0.128	0.005	5272	-23.4	<0.001
$SPEI_{Dr}$	0.136	0.008	5271	16.3	<0.001
$SPEI_{PostDr}$	0.185	0.008	5271	23.7	<0.001
Spatial autocovariate					
RAC	0.817	0.005	5271	173.2	<0.001

Abbreviations: Ar, aridity; Dl, local deforestation index (forest structure); Ar:Dl, Ar-Dl interaction; $SPEI_{PreDr}$, pre-drought SPEI; $SPEI_{Dr}$, drought event SPEI; $SPEI_{PostDr}$, post-drought SPEI; RAC, residual autocovariate; St. β, standardized coefficients; S.E., standard error; d.f., degrees of freedom.

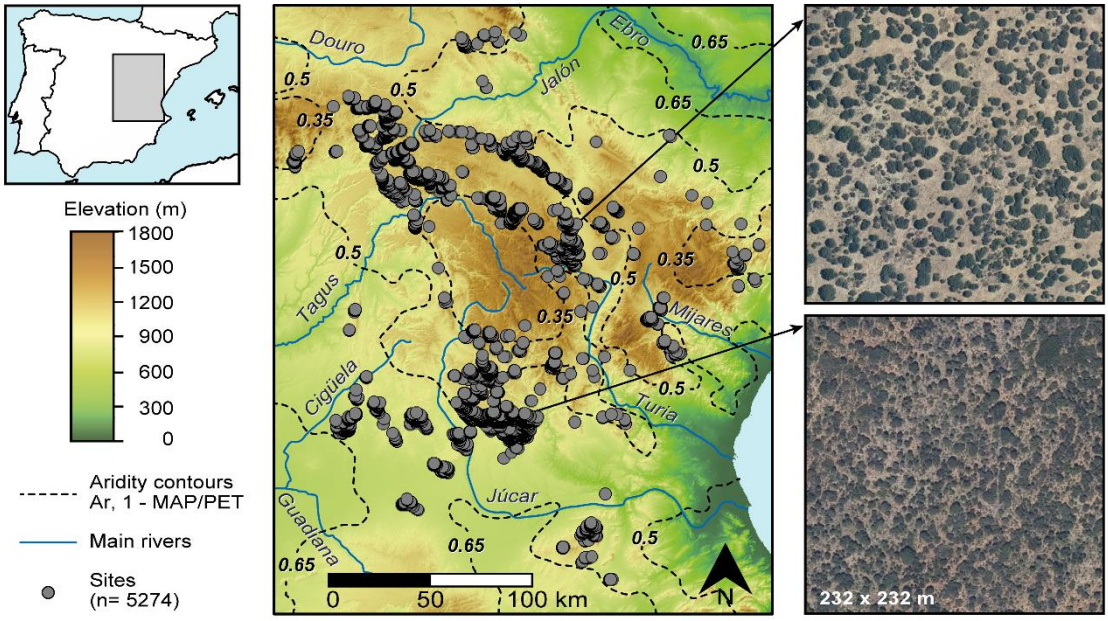

Figure 1. Location map (total 5274 sites) and aerial view (0.5 m resolution images of the Spanish National Orthophoto Program) of two *Quercus ilex* woodland sites (each 232 × 232 m size). Ar represents climate aridity (calculated as 1 - MAP/PET, where MAP and PET are mean annual precipitation and potential evapotranspiration, respectively).

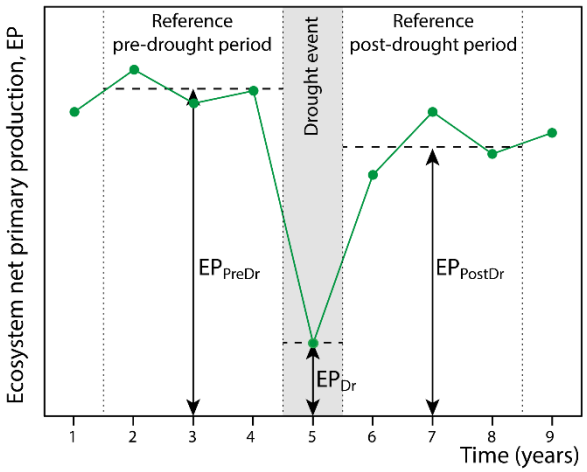

Figure 2. Schematic representation of the annual dynamics and response of ecosystem net primary production (EP) to the effects of a drought event. EP_{PreDr}, EP_{Dr} and EP_{PostDr} represents pre-drought, drought and post-drought net primary production, respectively.

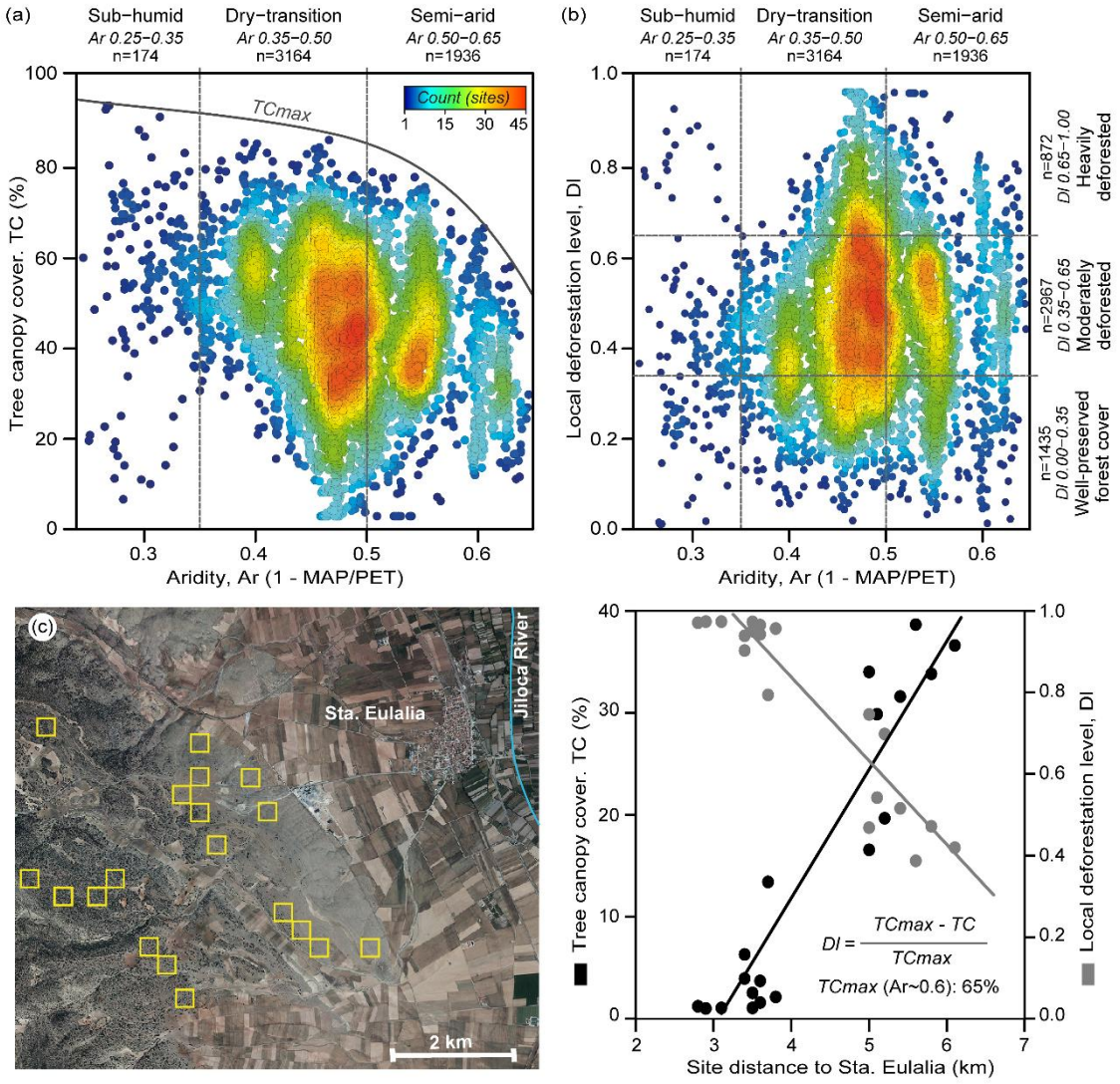

Figure 3. Forest structure and its relationship to climate aridity and the legacy of human use in the analyzed *Quercus ilex* woodlands: distribution of (a) tree canopy cover (TC, %) and (b) local deforestation level (Dl) of the study sites along the explored climate aridity gradient; (c) tree canopy cover and local deforestation level variations in a set of 19 *Q. ilex* sites distributed at increasing distances from a rural settlement in the study region (Santa Eulalia, Teruel). The envelope TC_{max} (%) line in (a) represents maximum tree cover along the climate aridity range of the study holm oak sites. The aerial view (Spanish National Orthophoto Program) and TC-Dl spatial trends in (c) are adapted form Moreno-de-las-Heras et al. (2018).

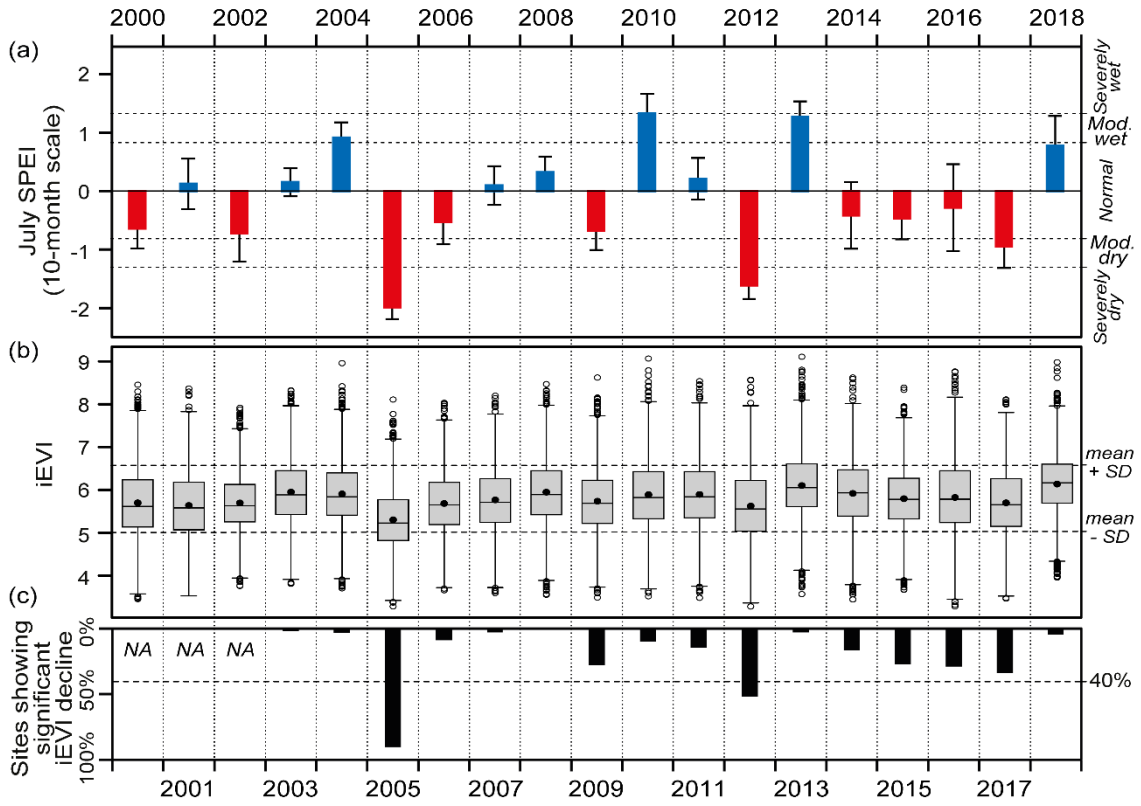

Figure 4. Drought conditions and ecosystem production along 2000-2019 for the studied *Quercus ilex* woodlands: (a) mean ± SD hydric conditions (10-month scale July SPEI; blue and red colors indicate wet and dry conditions, respectively); (b) ecosystem production (iEVI); (c) proportion of sites showing significant drought impacts on ecosystem production (i.e., iEVI of present annual cycle is lower than mean minus one SD iEVI of the reference, three previous years). Classification of (severely, moderately) wet/dry and normal hydric conditions in (a) follows Liberato et al. (2021). NA in (c) indicates that iEVI decline was not evaluated for 2000-2002 (reference period is shorter than three years).

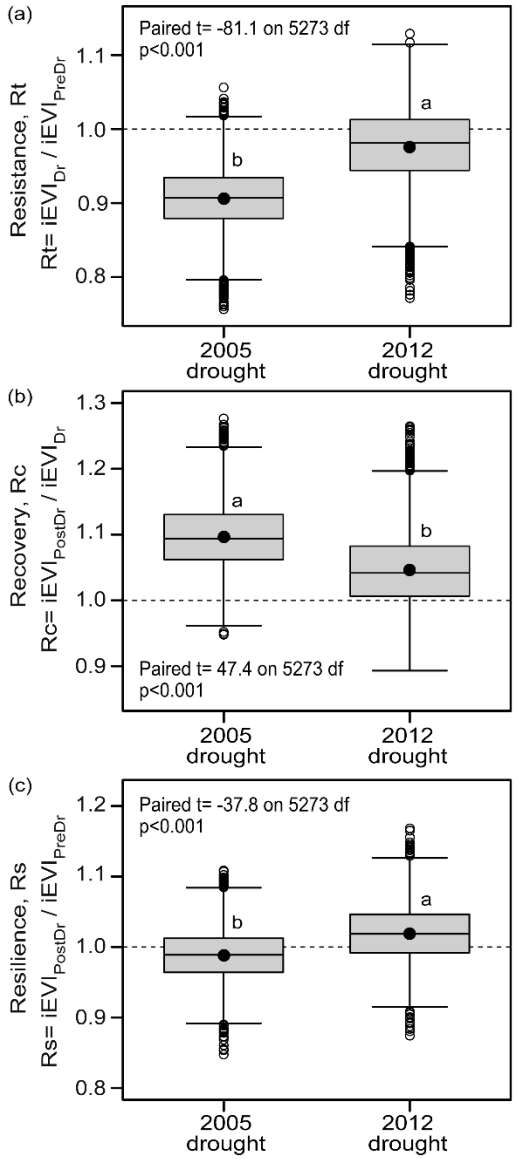

Figure 5. Responses of the study *Quercus ilex* sites to the 2005 and 2012 extreme drought episodes: between drought comparisons of (a) drought resistance (Rt), (b) recovery (Rc), and (c) resilience (Rs). Different letters indicate statistical differences between drought events (tested using paired t tests). $iEVI_{PreDr}$, $iEVI_{Dr}$ and $iEVI_{PostDr}$ in the (Rt, Rc and Rs) equations indicate pre-drought, drought and post-drought ecosystem production, respectively.

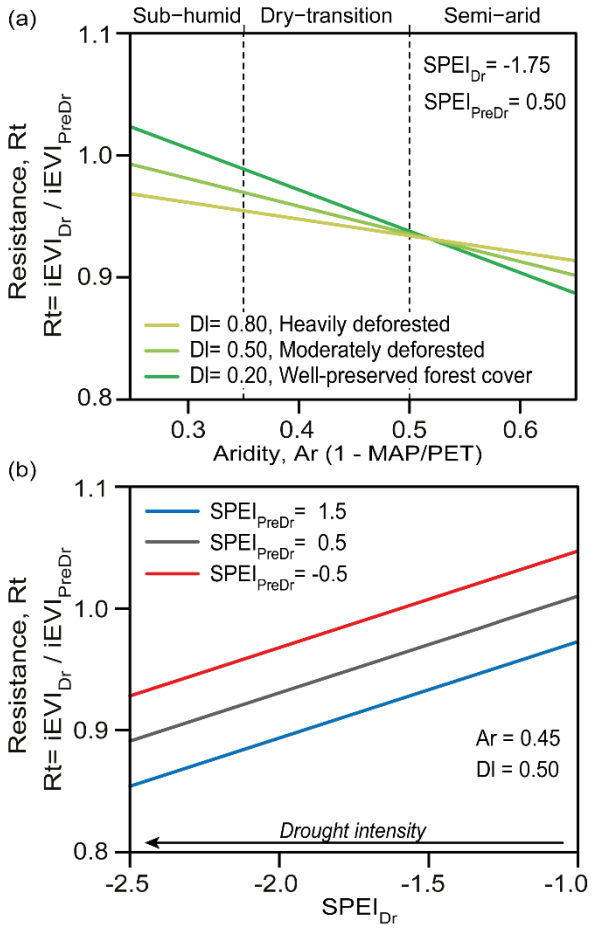

Figure 6. Controlling factors of *Quercus ilex* woodland resistance to drought (Rt): (a) linear mixed model (LMM) effects of climate aridity (Ar) and forest structure (Dl, local deforestation index); (b) LMM effects of drought event SPEI ($SPEI_{Dr}$) and pre-drought SPEI ($SPEI_{PreDr}$). $iEVI_{Dr}$ and $iEVI_{PreDr}$ in the Rt equation indicate drought and pre-drought ecosystem production, respectively.

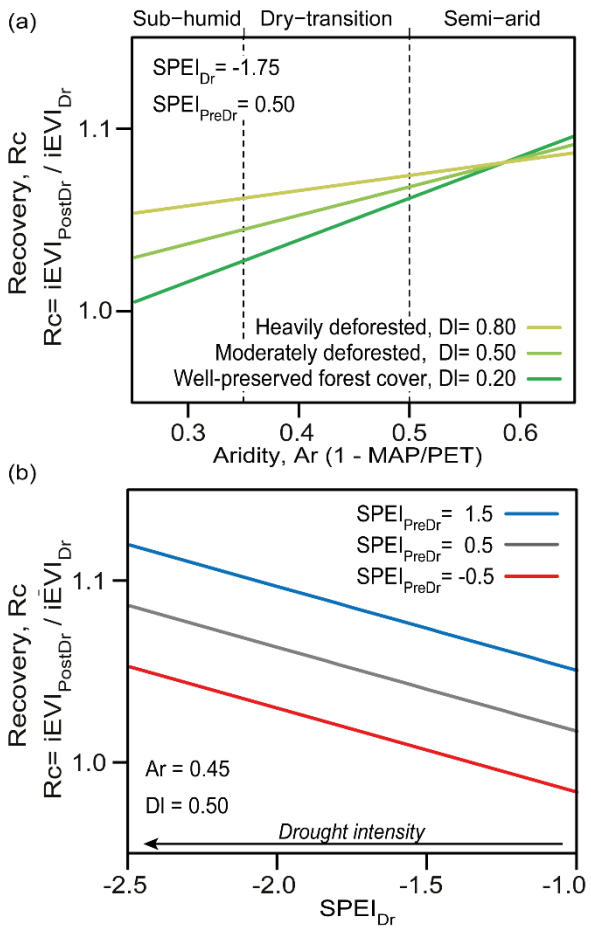

Figure 7. Controlling factors of *Quercus ilex* woodland recovery to drought (Rc): (a) linear mixed model (LMM) effects of climate aridity (Ar) and forest structure (Dl, local deforestation index); (b) LMM effects of drought event SPEI ($SPEI_{Dr}$) and pre-drought SPEI ($SPEI_{PreDr}$). $iEVI_{PostDr}$ and $iEVI_{Dr}$ in the Rc equation indicate post-drought and drought ecosystem production, respectively.

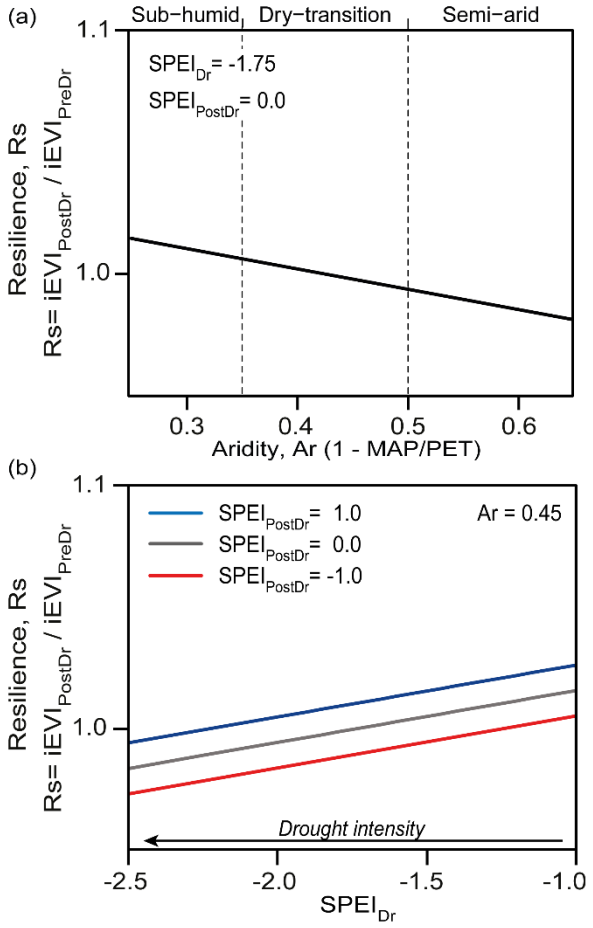

Figure 8. Controlling factors of *Quercus ilex* woodland resilience to drought (Rs): (a) linear mixed model (LMM) effects of climate aridity (Ar); (b) LMM effects of drought event SPEI ($SPEI_{Dr}$) and post-drought SPEI ($SPEI_{PostDr}$). $iEVI_{PostDr}$ and $iEVI_{PreDr}$ in the Rs equation indicate post-and pre-drought ecosystem production, respectively.